



# How does roughness kill adhesion?

L. Afferrante<sup>a,\*</sup>, G. Violano<sup>a,b</sup>, D. Dini<sup>c</sup>

<sup>a</sup> Department of Mechanics, Mathematics and Management, Polytechnic University of Bari, Via E. Orabona, 4, 70125, Bari, Italy

<sup>b</sup> Department of Materials Science and Engineering, Saarland University, 66123 Saarbrücken, Germany

<sup>c</sup> Department of Mechanical Engineering, Imperial College London, London SW7 2AZ, United Kingdom

## ARTICLE INFO

### Keywords:

Adhesion  
Roughness  
Contact mechanics  
Lennard-Jones potential

## ABSTRACT

It is well-known that adhesion is strongly influenced by surface roughness. Nevertheless, the literature currently contains an ongoing debate regarding which roughness scales are primarily responsible for adhesion loss. In this study, we aim to contribute to this debate by conducting numerical simulations on self-affine fractal profiles with varying fractal dimensions.

Our results reveal that the long-wavelength portion of the roughness spectrum plays a crucial role in killing adhesion when considering profiles with Hurst exponent  $H > 0.5$ . Conversely, for profiles with  $H < 0.5$ , results show a different trend, indicating that adhesive stickiness is also influenced by short wavelength roughness. These findings are corroborated by our recent experimental observations. In such case, adhesive hysteresis and pull-off force exhibit a continuous decrease with increasing roughness scales. However, for  $H > 0.5$ , the pull-off force converges towards a finite value as the magnification increases.

## 1. Introduction

Van der Waals interactions between surface atoms produce attractive tractions that are strong on a macroscopic scale (orders of magnitude larger than atmospheric pressure (Pastewka and Robbins, 2014)), but we seldomly observe objects stick strongly together. What is the reason of this adhesion paradox? All surfaces that appear smooth at the macro and mesoscopic level always present a certain degree of roughness at the micro and nanoscopic level (Tiwari et al., 2020; Jacobs et al., 2013; Dalvi et al., 2019).

There is a large debate in the scientific community (Pastewka and Robbins, 2014; Violano et al., 2019a; Wang and Müser, 2022; Thimons et al., 2021) on which roughness scales kill adhesion and which roughness parameters characterize the surface stickiness, i.e. “the possibility of sustaining macroscopic tensile pressures or else non-zero contact area without load” (Violano et al., 2021b). The above questions are of great industrial interest, as adhesion-control with surface texturing and topography manipulation are exploited, for example, in biomaterials (Xu and Siedlecki, 2012), microelectromechanical systems (DelRio et al., 2005; Komvopoulos, 2003), coatings (Kromer et al., 2018), soft grippers (Tian et al., 2019).

In the first scientifically organized work aimed at studying the effect of surface roughness on adhesion, Fuller and Tabor (1975) showed through experiments that small surface roughnesses can produce a large reduction in adhesion. Specifically, they found adhesion is mainly impaired by long wavelength roughness, which is related to the RMS roughness amplitude  $h_{\text{rms}}$ .

In theoretical-experimental investigations, Peressadko et al. (2005) found no specific relation between adhesion and RMS amplitude  $h_{\text{rms}}$ . On the contrary, they suggested the main roughness quantity affecting adhesion is the second moment of the surface power spectral density (PSD), which is related to the RMS of the surface slopes  $h'_{\text{rms}}$ . Similar outcomes were found in numerical studies by Pastewka & Robbins (PR) (Pastewka and Robbins, 2014) and Müser (2016), who identified local stickiness

\* Corresponding author.

E-mail address: [luciano.afferrante@poliba.it](mailto:luciano.afferrante@poliba.it) (L. Afferrante).

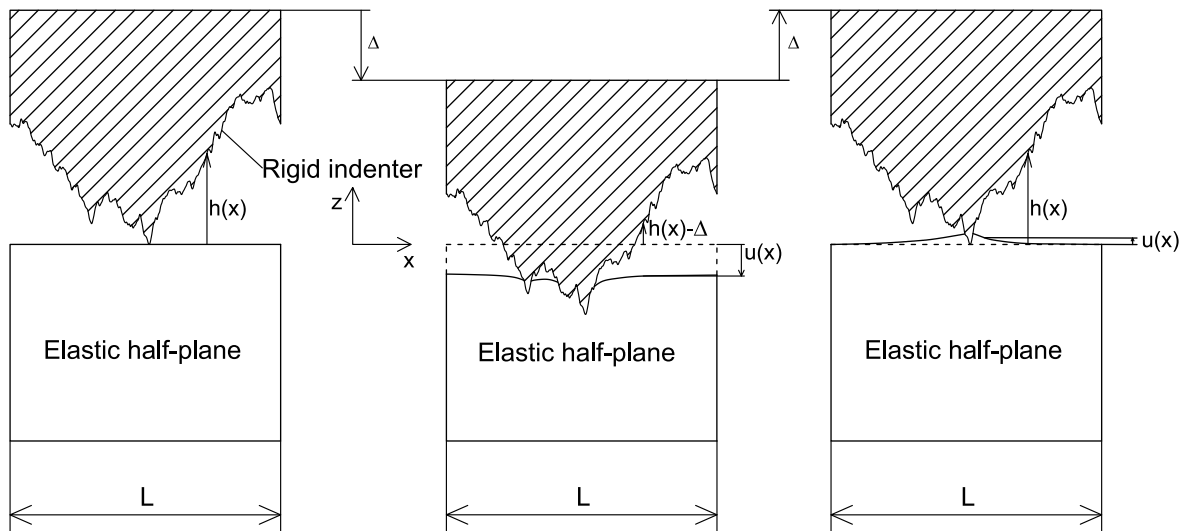


Fig. 1. The problem under investigation: a rigid randomly rough 1D profile is pressed into a linear elastic half-plane and then pulled apart from it.

criteria depending on the small scale roughnesses. Specifically, PR showed stickiness is met when the total adhesive force is larger than the total repulsive one. However, such criterion is based on the assumption that interactions act as in single-asperity contacts with long-range adhesion.

PR *local* stickiness criterion is clearly in contrast with FT findings that instead show adhesion is mainly affected by the RMS amplitude of roughness. In this regard, recent theoretical works showed the pull-off force, i.e., the maximum tensile force required to detach the surfaces, does not depend on local slopes and curvature (Ciavarella, 2018; Joe et al., 2017, 2018).

An advanced multisasperity approach has been developed by Violano & Afferrante (Violano and Afferrante, 2019b,a; Violano et al., 2019b), who showed that the adhesive interactions are influenced only by  $h_{\text{rms}}$ , while the RMS surface gradient  $h'_{\text{rms}}$  only affects the non-adhesive contact force. On the basis of such findings, Violano et al. (2019a) derived a new stickiness criterion in the framework of Persson & Scaraggi (PS) theory (Persson and Scaraggi, 2014). They showed that for self-affine fractal surfaces with low fractal dimension ( $D < 2.5$ ), stickiness depends on the low wavelength cut-off of roughness and RMS amplitude  $h_{\text{rms}}$ , which are well-defined *global* quantities. These results find confirmation in recent experimental investigations of Tiwari et al. (2020), which show that “adhesion in most cases is killed by the longest-wavelength roughness”.

Therefore, for rough surfaces with low fractal dimension  $D (< 2.5)$ , there is a certain agreement on the fact that stickiness is quite independent of the upper truncation frequency of the roughness spectrum (Ciavarella, 2020), and hence of the local roughness parameters. However, for high fractal dimension  $D (> 2.5)$  less data are available in the literature.

In a recent theoretical work, Violano et al. (2021b) argued that for high  $D$ , “stickiness is more influenced by short wavelength roughness with respect to the low  $D$  case”. This conclusion is not in contrast with the results reported in Salehani et al. (2020), where fully numerical calculations, performed on 1D fractal profiles show that, for high  $D$ , the smaller wavelengths influence the adhesive behaviour as the real contact area decreases with increasing the fractal discretization and hence the RMS surface slope  $h'_{\text{rms}}$ . Moreover, recent experiments (Violano et al., 2023) have shown that, at high  $D$ , small wavelength roughness reduces adhesion.

Finally, in a recent work, Wang and Müser (2022) emphasized the importance of a *global* energy analysis for the assessment of stickiness (Violano et al., 2019a; Ciavarella, 2020) over purely *local* stickiness criteria (Pastewka and Robbins, 2014; Müser, 2016).

Moving from the aforementioned context, we herein present a numerical model to perform adhesive contact simulations on 1D self-affine fractal rough profiles. We aim at investigating the effect of long and small scale roughness in the case of high and low fractal dimensions. We discuss our findings in the light of experiments recently performed and reported in Violano et al. (2023).

## 2. The model

The problem under investigation is sketched in Fig. 1, where a rigid randomly rough 1D profile is pressed into a linear elastic half-plane and then pulled apart from it. Investigating 1D profiles is effective as they can be considered a good approximation of the anisotropic surfaces that are usually obtained after machine tooling (Thomas, 1998). Moreover, as shown in Scaraggi et al. (2013), one can use a simple criterion to make a 2D isotropic rough surface equivalent to a 1D one, from the point of view of contact area and separation, by replacing the power spectral density of the original 2D surface with an equivalent power spectral density of a 1D rough profile. For this reason, analysing 1D profiles can be a profitable strategy to reduce the computational cost typical of 2D rough surfaces.

The rough profile is assumed to be periodic with period  $L$  to avoid size effects due to lateral boundaries. The quantities  $h$  and  $u$  are respectively the heights distribution of the rough profile and the interfacial normal displacement of the elastic half-plane occurring when it is squeezed of  $\Delta$  by the rigid indenter.

To describe the rough profile, we adopt a self-affine fractal geometry with a power spectral density (PSD) which depends on the wavenumber  $q$  according to

$$\begin{aligned} C(q) &= C_0 \quad \text{for} \quad q_L \leq q < q_r \\ C(q) &= C_0 (q/q_r)^{-(1+2H)} \quad \text{for} \quad q_r \leq q < q_s \end{aligned} \quad (1)$$

and zero otherwise. We have denoted with  $q_L = 2\pi/L$  and  $q_s = 2\pi/\lambda_s$  the short and long frequencies cut-off, respectively, while  $q_r = 2\pi/\lambda_r$  is the roll-off frequency. The parameter  $H$  is the so-called Hurst exponent, which is related to the fractal dimension through the relation  $D = 2 - H$ .

The rough profile of the indenter is hence described by the Fourier series

$$h(x) = \sum_{k=1}^N h_k \cos(kq_L x + \varphi_k) \quad (2)$$

where the amplitudes  $h_k$  and phases  $\varphi_k$  are determined in such a way that the resulting profile is Gaussian (more details about the numerical generation of the profile can be found in Putignano et al. (2012), Bottiglione and Carbone (2013)).

To study the above problem, a Finite Element (FE) model has been developed based on the approach presented in Afferrante and Violano (2022b,a). The adhesive interactions are modelled exploiting the Derjaguin approximation (Derjaguin, 1934), which allows to calculate the force between two bodies of arbitrary shape from the interaction free energy between two planar surfaces. Therefore, “while the surface force between two planar half-spaces is by symmetry a normal traction, between curved surfaces it is necessary to assume that the tractions are normal to the surface, or more specifically, that any tangential tractions have no effect” (Greenwood, 2009). Moreover, we make use of nonlinear spring elements with a traction–displacement relation based on the assumption that Lennard-Jones potential law defines the interaction between the molecules of the indenter and the half-plane,

$$\sigma(x) = \frac{8\Delta\gamma}{3\epsilon} \left[ \left( \frac{\epsilon}{g(x)} \right)^3 - \left( \frac{\epsilon}{g(x)} \right)^9 \right] \quad (3)$$

where  $g(x)$  is the interfacial gap,  $\Delta\gamma$  the surface energy of adhesion, and  $\epsilon$  the range of action of van der Waals forces.

During the approach of the indenter, multiple snap-through events occur due to the attractive forces. To prevent instability and, hence, numerical convergence difficulties, the static problem is runned as a “slow dynamic” analysis with dashpot and mass elements positioned at the interface (we used point masses of  $10^{-5}$  kg and dashpots with a damping constant  $10^{12}$  kg/s). In addition, proper time-integration parameters are used to prevent divergence (a time step increment  $\Delta t = 0.1$  s was used except in cases of contact instability where the time step is reduced by up to 1000 times). Notice damping and inertia forces do not alter the contact solution as they activate only during the snap-through events.

### 3. Results and discussion

All simulations have been carried out for a nearly incompressible elastic material ( $\nu = 0.49$ ) with Young’s modulus  $E \simeq 380$  MPa and a surface energy  $\Delta\gamma = 0.05$  J/m<sup>2</sup>. Also, we have considered self-affine profiles characterized by wavenumber cut-off  $q_L = 2\pi/L \approx 1.5708 \times 10^6$  m<sup>-1</sup> and roll-off  $q_r = 2\pi/\lambda_r \approx 3.1416 \times 10^6$  m<sup>-1</sup> with RMS roughness amplitude  $h_{\text{rms}}$  in the range  $5 \div 50$  nm. Moreover, profiles with magnifications (i.e., number of scales)  $\zeta$  ranging between  $64 \div 256$  ( $64 \div 2048$  for  $h_{\text{rms}} = 20$  nm) have been generated, being  $\zeta = q_s/q_L$  and  $q_s$  the wavenumber cut-off at high frequencies (small wavelengths). As a result, the RMS of the surface slopes  $h'_{\text{rms}}$  ranges from a minimum of about 0.037 for  $H = 0.8$  and  $h_{\text{rms}} = 5$  nm with  $\zeta = 64$ , to a maximum of about 1.8 for  $H = 0.4$  and  $h_{\text{rms}} = 50$  nm with  $\zeta = 256$ . Finally, we recall that, in the generation of the profiles the same random phase distribution is maintained when the magnification is changed.

The curves of Fig. 2 show the area–load response obtained for various RMS roughness amplitude  $h_{\text{rms}}$ , considering high (Fig. 2a) and low (Fig. 2b) fractal dimensions. In the present context, a rigorous definition of the contact area is not feasible due to the presence of a non-zero gap at the interface. Consequently, the contact area is defined as the sum of the segments where the gap is below a specified threshold, ensuring that the interactions between the surfaces, whether repulsive or attractive, fall within a certain tolerance. In the specific case, contact is assumed to occur when  $(g(x) - \epsilon)/\epsilon < 0.1$ .

Fig. 2 illustrates a loading–unloading cycle, where unloading always commences after achieving complete contact. In both cases, for high and low fractal dimension, roughness-induced adhesive hysteresis is observed, as evidenced by the deviation of the unloading path from the loading path. This observation aligns with previous numerical (Carbone et al., 2015; Medina and Dini, 2014) and experimental studies (Dalvi et al., 2019). Additionally, it is noted that rough profiles with a lower fractal dimension exhibit greater stickiness.

As expected, increasing the RMS roughness amplitude  $h_{\text{rms}}$  requires higher loads to achieve the same contact area and the pull-off stress  $\sigma_{\text{pull-off}}$  significantly reduces, eventually vanishing at higher RMS roughness amplitude. This behaviour is clearly illustrated in Fig. 3, where  $\sigma_{\text{pull-off}}$  is plotted against  $h_{\text{rms}}$ . Therefore, considering that  $h_{\text{rms}}$  mainly depends on long wavelengths, we can state that the long scale roughness always suppresses adhesion. This result is not new and agrees with the pioneering experimental data of Fuller and Tabor (1975), more recent studies of Tiwari et al. (2020), Violano et al. (2021a), and numerous theoretical works on this topic (Violano et al., 2019a; Joe et al., 2017; Ciavarella, 2020; Salehani et al., 2020). Some exceptions have been observed experimentally for (sub)nanometric roughnesses (Deng and Kesari, 2019), where an optimal value of  $h_{\text{rms}}$  may exist that maximizes the pull-off force. This behaviour is also shown by Medina and Dini (2014), who performed numerical simulations on 2D contacts.

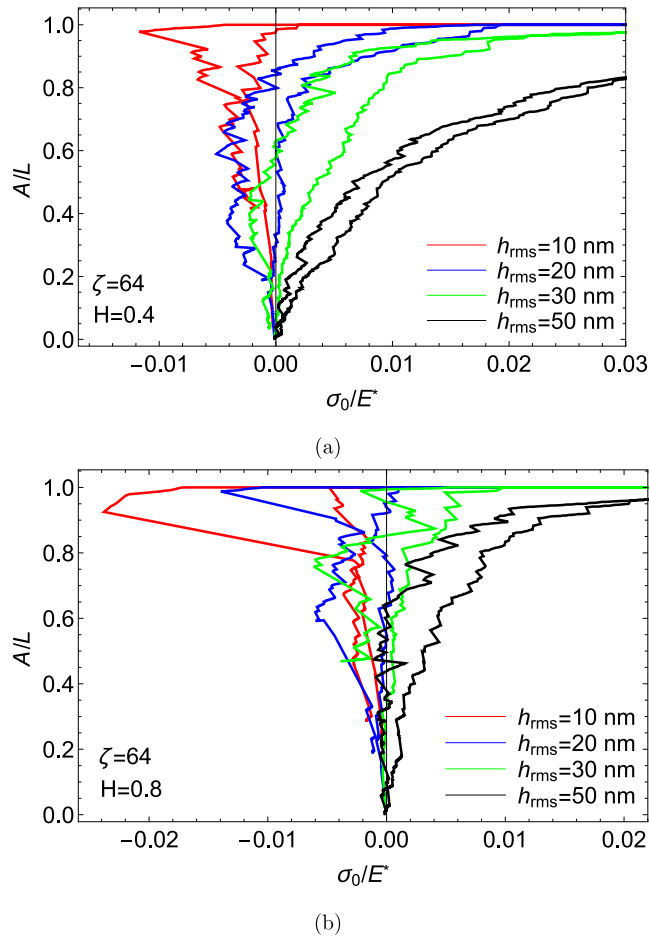


Fig. 2. The normalized contact area  $A/L$  as a function of the applied contact pressure  $\sigma_0/E^*$  for different values of the RMS roughness amplitude  $h_{rms}$ . Results are given for self-affine fractal profiles with  $\zeta = 64$  and Hurst exponent  $H = 0.4$  (Fig. 2a) and  $H = 0.8$  (Fig. 2b).

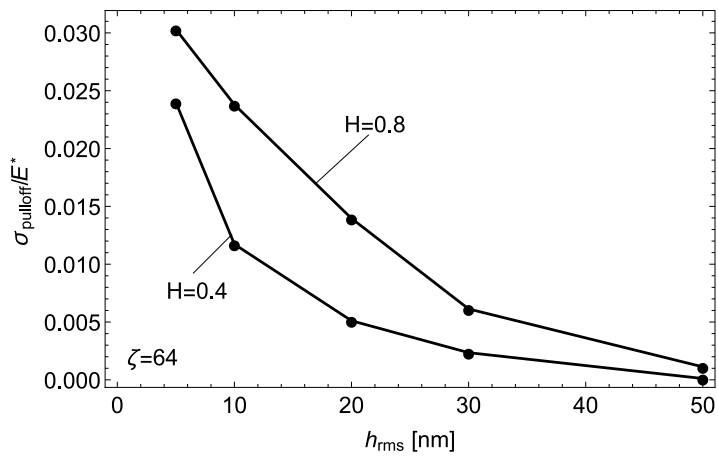


Fig. 3. The pull-off stress as a function of the RMS roughness amplitude  $h_{rms}$ . Results are given for self-affine fractal profiles with magnification  $\zeta = 64$  and Hurst exponent  $H = 0.4$  and  $H = 0.8$ .

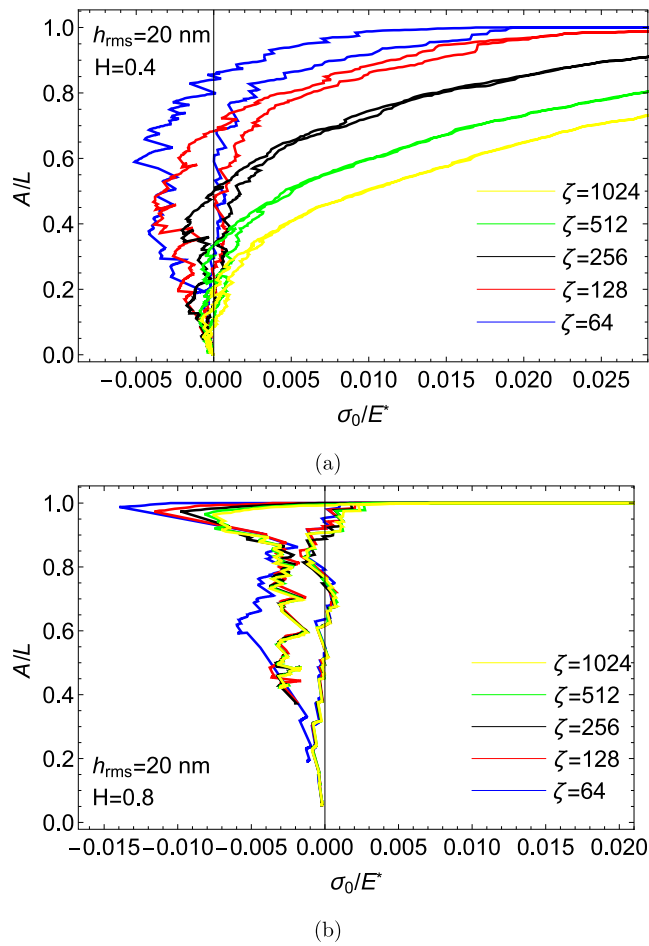


Fig. 4. The normalized contact area  $A/L$  as a function of the applied contact pressure  $\sigma_0/E^*$  for different values of the magnification  $\zeta$ . Results are given for self-affine fractal profiles with RMS roughness amplitude  $h_{rms} = 20$  nm and Hurst exponent  $H = 0.4$  (Fig. 4a) and  $H = 0.8$  (Fig. 4b).

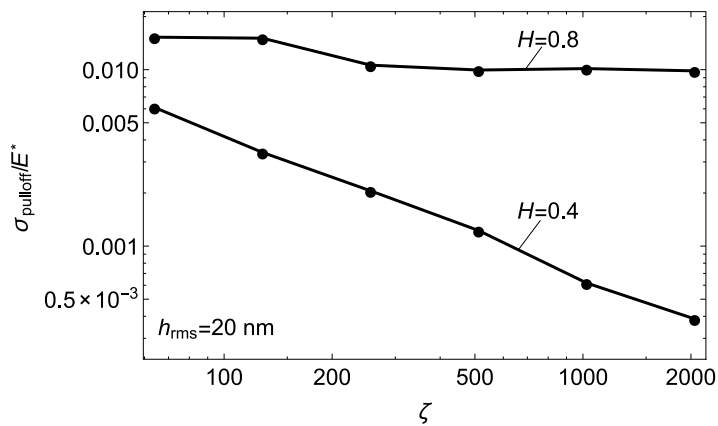


Fig. 5. The pull-off stress as a function of the magnification  $\zeta$  on a double logarithmic scale. Results are given for self-affine fractal profiles with RMS roughness amplitude  $h_{rms} = 20$  nm and Hurst exponent  $H = 0.4$  and  $H = 0.8$ .

They explained that for (sub)nanometric roughness “the small amount of roughness causes a large region within the macro contact to experience a small degree of separation, where the adhesive force is maximum.” However, as the roughness further increases, “the majority of the potential contact region is separated by greater distances and experiences low adhesive forces”.

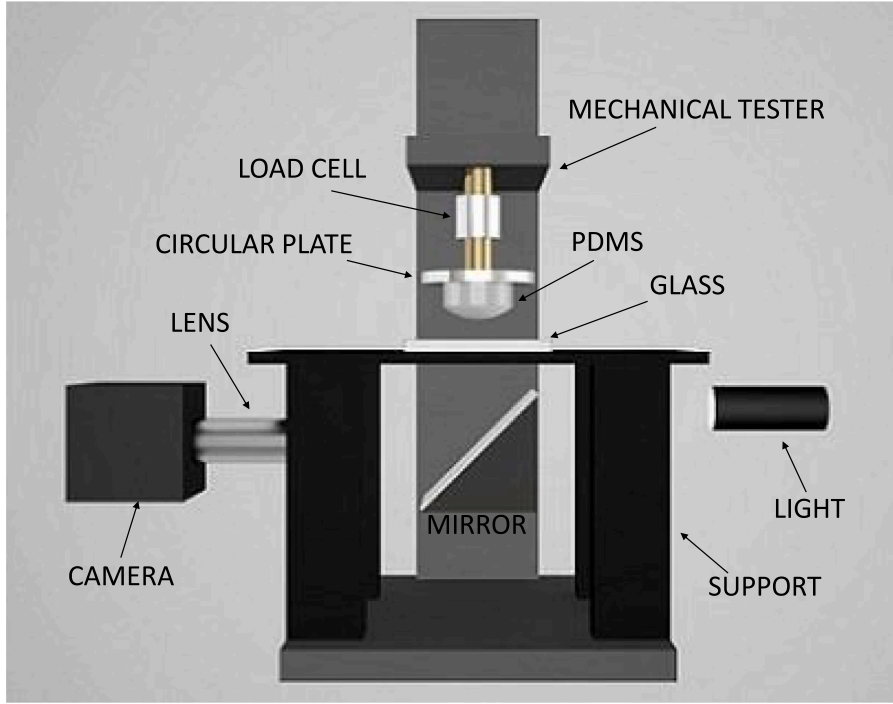


Fig. 6. The experimental equipment used to perform JKR-like experiments (Violano et al. (2023)). Three PDMS indenters were used in the tests. Two samples showed very similar values of Young's moduli ( $E = 1.916$  MPa and  $E = 1.903$  MPa, respectively) and surface energies ( $\Delta\gamma = 591$  mJ/m<sup>2</sup> and  $\Delta\gamma = 608$  mJ/m<sup>2</sup>, respectively). The third sample showed lower values ( $E = 1.746$  MPa and  $\Delta\gamma = 382$  mJ/m<sup>2</sup>) because of differences occurred during the components mixing and casting. More details about the experimental set-up can be found in Violano et al. (2023).

More controversial is the question about the influence of small scale roughness on the adhesion. Therefore, to investigate the effect of high spatial frequencies of roughness on adhesion, we conducted simulations on profiles with the same content of long wavelength roughness (i.e., identical  $h_{\text{rms}}$ ), but different magnifications  $\zeta$  (corresponding to different  $h'_{\text{rms}}$ ). The results are presented in Fig. 4, where the relative contact area is plotted as a function of the applied pressure for  $h_{\text{rms}} = 20$  nm, various values of  $\zeta$ , and  $H = 0.4$  (Fig. 4a) and  $H = 0.8$  (Fig. 4b). Similar to Fig. 2, unloading always starts after achieving full contact.

For  $H = 0.8$  ( $D < 1.5$ ), the loading curve is found to be independent of the fractal magnification, as reported in Salehani et al. (2020). This independence also extends to the unloading path at higher magnifications, as the unloading curves tend to overlap for  $\zeta > 512$ . Hence, it can be concluded that the contact behaviour is essentially unaffected by the smallest wavelengths.

In contrast, for  $H = 0.4$  ( $D > 1.5$ ), the contact behaviour undergoes significant changes and becomes highly dependent on the smallest scale roughness. The contact area and the adhesive hysteresis increase with reducing  $\zeta$ , indicating that a smoother surface exhibits stronger adhesion to the substrate.

Notably, for  $H = 0.8$ , the pull-off force and energy hysteresis remain finite even at increased magnification. Conversely, for  $H = 0.4$ , hysteresis and pull-off force decrease with the magnification. Consequently, in the latter case, the smallest wavelengths have a pronounced impact on adhesion, demonstrating its dependence on local slopes and curvature.

In this regard, Fig. 5 illustrates the pull-off stress  $\sigma_{\text{pull-off}}$  as a function of the magnification  $\zeta$  on a double logarithmic scale at fixed  $h_{\text{rms}} = 20$  nm and  $H = 0.4, 0.8$ . While definitive conclusions cannot be drawn from the curves in Fig. 5, it appears that for  $H = 0.8$ ,  $\sigma_{\text{pull-off}}$  converges to a finite value, whereas it monotonically decreases with increasing  $\zeta$  for  $H = 0.4$ . This behaviour is in line with the recent findings of Wang and Müser (2022), who observed that the pull-off force decreases with the reduced surface energy  $\Delta\hat{\gamma} = \Delta\gamma/U_{\text{el,fc}}$ , where  $U_{\text{el,fc}}$  denotes the elastic energy in full contact. Specifically, as for  $\zeta \rightarrow \infty$ ,  $U_{\text{el,fc}}$  diverges when  $H < 0.5$ , but converges to a finite value when  $H > 0.5$ . In the former case,  $\Delta\hat{\gamma}$  tends to zero, while in the latter case, it remains finite. Consequently, a similar behaviour can be expected for the pull-off force since  $\sigma_{\text{pull-off}}$  is closely related to  $\Delta\hat{\gamma}$ .

Our conclusions are also consistent with our recent experimental findings reported in Violano et al. (2023), where JKR-like tests were conducted on glass rough substrates, with a focus on high fractal dimension.

Fig. 6 shows the experimental set-up used in the tests. Specifically, Polydimethylsiloxane spherical indenters (PDMS, Sylgard 184, Dow Corning) with standard mixing ratio (10 : 1) of base and cross-linking agent were used in all the experiments. Adhesion tests were carried out on four glass substrates (TECHSPEC-4 N-BK7 Precision Windows) with a thickness  $t = 4$  mm, Young's modulus  $E = 82$  GPa, and Poisson's ratio  $\nu = 0.206$ .

To examine the effects of topographical changes on adhesion, the surface roughness characteristics of the substrates were conveniently modified. Thus, one specimen was left untreated, considered nominally smooth, while the surface roughness properties

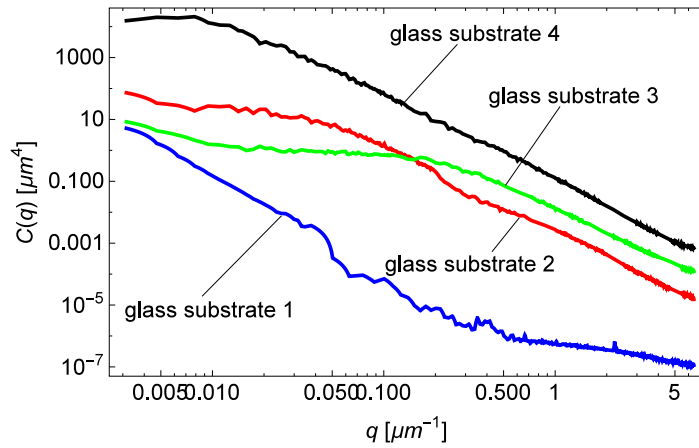
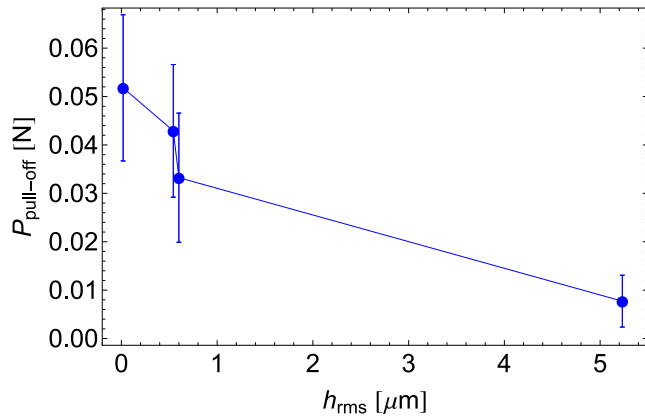
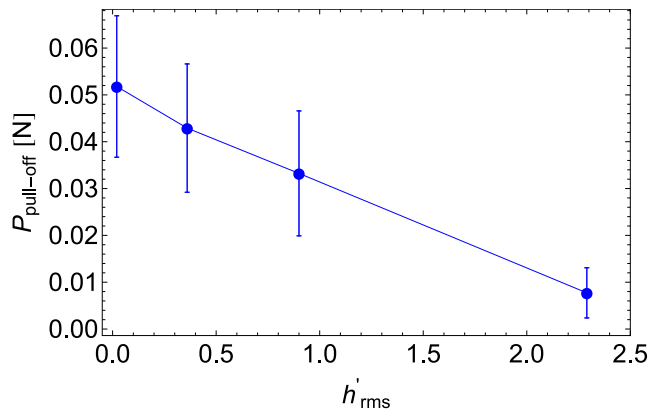


Fig. 7. The power spectral density  $C(q)$  of the surface height distribution for the glass substrates used in JKR-like experiments (Violano et al. (2023)).



(a)



(b)

Fig. 8. The pull-off force as a function of the (a) RMS roughness amplitude and (b) RMS surface slope. We show the average pull-off force obtained from the tests performed in Violano et al. (2023). Error bars denote the range of the results obtained.

of the other specimens were modified as follows: (i) specimen 2 underwent manual sanding with sandpaper P400, (ii) specimen 3 underwent fluid polishing, and (iii) specimen 4 underwent sandblasting. The surface roughness was then characterized by using the white light interferometer Wyko NT9100 - Veeco. Fig. 7 shows the power spectral density (PSD) for all rough substrates (specimens 2, 3, and 4), which present self-affine fractal surfaces with a Hurst exponent  $H$  of about 0.4 (Violano et al., 2023).



The results of the experiments, summarized in Fig. 8, confirm that adding roughness to a surface leads to a reduction in adhesion, as smaller pull-off forces are required to detach two adherent surfaces. The pull-off force data  $F_{\text{pull-off}}$  were calculated as the average of values obtained from JKR-like tests performed with the three PDMS spherical samples on the four glass substrates.

Interestingly, in this case, the surface adhesion is influenced by the finest scale roughness. The observed reduction in  $F_{\text{pull-off}}$  at constant  $h_{\text{rms}} \sim 0.55 \mu\text{m}$  is not attributed to the longest-wavelength roughness. Instead, this decrease in the pull-off force coincides with an increase in the small wavelength components of the roughness as  $h'_{\text{rms}}$  increases (see Fig. 8b). Consequently, for the high fractal dimension investigated here ( $H = 0.4$ ), the experimental data indicate that the small wavelength roughness kills adhesion and its influence is no longer negligible, which is in agreement with our numerical findings.

#### 4. Conclusions

Numerical simulations have been carried out on self-affine fractal profiles to explore the role of roughness in the adhesive behaviour of contacting bodies. The objective is to understand which roughness scales control the rupture of adhesive bonds.

The results show a strong dependence on the fractal dimension of the surfaces. Fractal profiles with Hurst exponent  $H = 0.8$  exhibit a negligible sensitivity to small-wavelength roughness, while profiles with Hurst exponent  $H = 0.4$  show that adhesive stickiness is affected by the smallest scale roughness. These findings are consistent with recent experimental tests.

Our results suggest that, at high roughness scales, both hysteresis and pull-off force tend to converge to a finite value for surfaces with low fractal dimension ( $D < 1.5$ ), in agreement with the stickiness criteria derived in Violano et al. (2019a), Wang and Müser (2022), Ciavarella (2020).

For surfaces with high fractal dimension ( $D > 1.5$ ), adhesion hysteresis and pull-off force appear to decrease continuously with the magnification, in agreement with the stickiness criteria proposed by Wang and Müser (2022) and Persson-Tosatti (Violano et al., 2021b), and in contrast with Ciavarella's BAM theory, which predicts a finite value for the pull-off force (Violano et al., 2021b).

#### CRedit authorship contribution statement

**L. Afferrante:** Conceived the presented idea, Developed the theory, designed the computational model and contributed to the final manuscript. **G. Violano:** Conceived the presented idea, Discussed the results and contributed to the final manuscript. **D. Dini:** Conceived the presented idea, Discussed the results and contributed to the final manuscript.

#### Declaration of competing interest

The authors declare that they have no known competing financial interests or personal relationships that could have appeared to influence the work reported in this paper.

#### Data availability

Data will be made available on request.

#### Acknowledgements

Useful discussions with M. H. Müser and A. Wang are acknowledged. Moreover, LA and GV acknowledges the Italian Ministry of University and Research as this work was supported under the Programme "Department of Excellence, Italy" Legge 232/2016 (Grant No. CUP - D93C23000100001).

#### References

- Afferrante, L., Violano, G., 2022a. The adhesion of viscoelastic bodies with slightly wave surfaces. *Tribol. Int.* 174, 107726.
- Afferrante, L., Violano, G., 2022b. On the effective surface energy in viscoelastic hertzian contacts. *J. Mech. Phys. Solids* 158, 104669.
- Bottiglione, F., Carbone, G., 2013. Role of statistical properties of randomly rough surfaces in controlling superhydrophobicity. *Langmuir* 29 (2), 599–609.
- Carbone, G., Pierro, E., Recchia, G., 2015. Loading-unloading hysteresis loop of randomly rough adhesive contacts. *Phys. Rev. E* 92 (6), 062404.
- Ciavarella, M., 2018. A very simple estimate of adhesion of hard solids with rough surfaces based on a bearing area model. *Meccanica* 53 (1), 241–250.
- Ciavarella, M., 2020. Universal features in stickiness criteria for soft adhesion with rough surfaces. *Tribol. Int.* 146, 106031.
- Dalvi, S., Gujrati, A., Khanal, S.R., Pastewka, L., Dhinojwala, A., Jacobs, T.D., 2019. Linking energy loss in soft adhesion to surface roughness. *Proc. Natl. Acad. Sci.* 116 (51), 25484–25490.
- DelRio, F.W., de Boer, M.P., Knapp, J.A., David Reedy, E., Clews, P.J., Dunn, M.L., 2005. The role of van der waals forces in adhesion of micromachined surfaces. *Nat. Mater.* 4 (8), 629–634.
- Deng, W., Kesari, H., 2019. Depth-dependent hysteresis in adhesive elastic contacts at large surface roughness. *Sci. Rep.* 9 (1), 1–12.
- Derjaguin, B., 1934. Molekulartheorie der äußeren reibung. *Z. Phys.* 88 (9), 661–675.
- Fuller, K.N.G., Tabor, D., 1975. The effect of surface roughness on the adhesion of elastic solids. *Proc. R. Soc. A* 345 (1642), 327–342.
- Greenwood, J.A., 2009. Adhesion of small spheres. *Phil. Mag.* 89 (11), 945–965.
- Jacobs, T.D., Ryan, K.E., Keating, P.L., Grierson, D.S., Lefever, J.A., Turner, K.T., et al., 2013. The effect of atomic-scale roughness on the adhesion of nanoscale asperities: a combined simulation and experimental investigation. *Tribol. Lett.* 50 (1), 81–93.
- Joe, J., Scaraggi, M., Barber, J.R., 2017. Effect of fine-scale roughness on the tractions between contacting bodies. *Tribol. Int.* 111, 52–56.
- Joe, J., Thouless, M.D., Barber, J.R., 2018. Effect of roughness on the adhesive tractions between contacting bodies. *J. Mech. Phys. Solids* 118, 365–373.



- Komvopoulos, K., 2003. Adhesion and friction forces in microelectromechanical systems: mechanisms, measurement, surface modification techniques, and adhesion theory. *J. Adhes. Sci. Technol.* 17 (4), 477–517.
- Kromer, R., Costil, S., Verdy, C., Gojon, S., Liao, H., 2018. Laser surface texturing to enhance adhesion bond strength of spray coatings—cold spraying, wire-arc spraying, and atmospheric plasma spraying. *Surf. Coat. Technol.* 352, 642–653.
- Medina, S., Dini, D., 2014. A numerical model for the deterministic analysis of adhesive rough contacts down to the nano-scale. *Int. J. Solids Struct.* 51 (14), 2620–2632.
- Müser, M.H., 2016. A dimensionless measure for adhesion and effects of the range of adhesion in contacts of nominally flat surfaces. *Tribol. Int.* 100, 41–47.
- Pastewka, L., Robbins, M.O., 2014. Contact between rough surfaces and a criterion for macroscopic adhesion. *Proc. Natl. Acad. Sci.* 111 (9), 3298–3303.
- Peressadko, A.G., Hosoda, N., Persson, B.N.J., 2005. Influence of surface roughness on adhesion between elastic bodies. *PRL* 95, 124301.
- Persson, B.N.J., Scaraggi, M., 2014. Theory of adhesion: Role of surface roughness. *J. Chem. Phys.* 141 (12).
- Putignano, C., Afferrante, L., Carbone, G., Demelio, G., 2012. A new efficient numerical method for contact mechanics of rough surfaces. *Int. J. Solids Struct.* 49 (2), 338–343.
- Salehani, M.K., van Dokkum, J.S., Irani, N., Nicola, L., 2020. On the load-area relation in rough adhesive contacts. *Tribol. Int.* 144, 106099.
- Scaraggi, M., Putignano, C., Carbone, G., 2013. Elastic contact of rough surfaces: A simple criterion to make 2D isotropic roughness equivalent to 1D one. *WEAR* 297, 811–817.
- Thimons, L.A., Gujrati, A., Sanner, A., Pastewka, L., Jacobs, T.D., 2021. Hard-material adhesion: Which scales of roughness matter? *Exp. Mech.* 61 (7), 1109–1120.
- Thomas, T.R., 1998. Trends in surface roughness. *Int. J. Mach. Tools Manuf.* 38 (5–6), 405–411.
- Tian, H., Li, X., Shao, J., Wang, C., Wang, Y., Tian, Y., Liu, H., 2019. Gecko-effect inspired soft gripper with high and switchable adhesion for rough surfaces. *Adv. Mater. Interfaces* 6 (18), 1900875.
- Tiwari, A., Wang, J., Persson, B.N.J., 2020. Adhesion paradox: Why adhesion is usually not observed for macroscopic solids. *Phys. Rev. E* 102, 042803.
- Violano, G., Afferrante, L., 2019a. Contact of rough surfaces: Modeling adhesion in advanced multiscale models. *Proc. IMechE Part J: J. Eng. Tribol.* 233 (10), 1–9. <http://dx.doi.org/10.1177/1350650119838669>.
- Violano, G., Afferrante, L., 2019b. On DMT methods to calculate adhesion in rough contacts. *Tribol. Int.* 130, 36–42. <http://dx.doi.org/10.1016/j.triboint.2018.09.004>.
- Violano, G., Afferrante, L., Papangelo, A., Ciavarella, M., 2019a. On stickiness of multiscale randomly rough surfaces. *J. Adhes.* 97 (6), 509–527.
- Violano, G., Chateauminis, A., Afferrante, L., 2021a. Rate-dependent adhesion of viscoelastic contacts, part II: Numerical model and hysteresis dissipation. *Mech. Mater.* 158, 103884.
- Violano, G., Demelio, G., Afferrante, L., 2019b. A note on the effect of surface topography on adhesion of hard elastic rough bodies with low surface energy. *J. Mech. Behav. Mater.* 28 (1), 8–12.
- Violano, G., Dini, D., Di Bari, A., Afferrante, L., 2023. Effect of roughness small scales on the adhesion of randomly rough surfaces with high fractal dimension. In: *IOP Conference Series: Materials Science and Engineering*. Vol. 1275, (1), IOP Publishing, 012024.
- Violano, G., Papangelo, A., Ciavarella, M., 2021b. Stickiness of randomly rough surfaces with high fractal dimension: is there a fractal limit? *Tribol. Int.* 159, 106971.
- Wang, A., Müser, M.H., 2022. Is there more than one stickiness criterion? *Friction* 1–13. <http://dx.doi.org/10.1007/s40544-022-0644-3>.
- Xu, L.C., Siedlecki, C.A., 2012. Submicron-textured biomaterial surface reduces staphylococcal bacterial adhesion and biofilm formation. *Acta Biomater.* 8 (1), 72–81.